PAPER *Special Section on 2006 International Symposium on Antennas and Propagation*

A Simple Mutual Coupling Compensation Technique in Array of Single-Mode Elements by a Weighted Mutual Coupling Matrix Based on the Impedance Matrix

Hiroyoshi YAMADA[†a)], ***Member***, **Masayuki MORISHITA**[††b)], ***Student Member***, ***and*** **Yoshio YAMAGUCHI**[†c)], ***Member***

SUMMARY High-resolution Direction-of-Arrival (DOA) estimation techniques for antenna arrays have been widely desired in many applications such as smart antennas, RF position location, and RFID system. To realize high-resolution capability of the techniques, precise array calibration is necessary. For an array of single-mode elements, a calibration matrix derived by the open-circuit method is the simplest one. Unfortunately, calibration performance of the method is not enough for the high-reslution DOA estimation techniques. In this paper, we consider problems of the calibration matrix derived by the method, and show that errors in the matrix can be effectively removed by an optimal diagonal weight coefficient. In the proposed compensation technique, the number of newly introduced parameters, or unknowns, is only one for an array of the identical elements. Performance of the simple compensation technique is verified numerically and experimentally.

key words: *array calibration, mutual coupling compensation, DOA estimation, superresolution technique*

1. Introduction

Recently, DOA (Direction Of Arrival) estimation based on antenna arrays has been expanding its application areas. For applications where number of array elements is limited, superresolution techniques, such as the MUSIC algorithm [1], are often required. However, array calibration is necessary to realize the high-resolution capability of the technique. The main causes for the performance deterioration are analogue component imbalance in the receiver(s), phase center (position) displacement of the array elements, and mutual coupling effects among the elements. The first two effects can be decreased by improving precision of the component and array, however, the latter effect, the mutual coupling, is unavoidable because it is a electromagnetic phenomenon caused by the array elements. In this paper, we focus on the mutual coupling compensation.

There are many array calibration techniques for the mutual coupling. The mutual coupling matrix estimation by using external reference plane waves will be a well-known calibration technique [2]. An extended technique for directional elements and/or their displacement of phase center can be found in [3]. This kind of methods can also decrease the coupling effect due to objects near the array, however, it would be often a hard task in some practical applications to carry out the calibration procedures.

For an array of single-mode elements without adjacent coupled objects, the open-circuit voltage method [4] is the well-known technique. This method has been proposed to compensate the effect of the mutual coupling by using the impedance matrix of the array elements including the load impedance. However, it has been pointed out that the method is only available for arrays with single-mode elements because the scattering effect of the elements in the open-circuit state is ignored [5]–[9]. Even a half-wavelength dipole is not the ideal single-mode element. To overcome this problem, Hui has proposed to use the estimated current distribution to include the open-circuit scattering effect into account [7]. Most of recent calibration techniques [5], [8]–[10] utilize the numerical results calculated by the method of moments (MoM). Also, concept of the mode expansion is used for the calibration of a microstrip array [11]. As discussed in these literatures, current distribution of the elements or numerical assistance by the MoM is required to realize the precise calibration.

However, the open-circuit method is still attractive for the arrays with quasi single-mode elements because the coupling error compensation can be done by using the impedance matrix which can be easily measured without any external reference waves. In this paper, we propose a simple coupling error compensation technique to improve the calibration performance of the open-circuit method. In the followings, we refer the open-circuit method as the conventional technique. Proposed modification is simple. It is just a diagonal weighting to the conventional coupling matrix derived in [4]. No information on the array/element shape is used in the proposed technique, then the technique will be said a 'compensation' technique. The technique will be only effective for the arrays of the quasi single-mode elements with moderate element separation.

Theoretical background of the proposed scheme is provided in Sect. 3. As described in this section, the proposed compensation matrix can be derived with rough approximations of coupling effect among the elements, however,

Manuscript received December 26, 2006.
Manuscript revised April 23, 2007.

[†]The authors are with the Graduate School of Science & Technology, Niigata University, Niigata-shi, 950-2181 Japan.
[††]The author is with the Faculty of Engineering, Niigata University, Niigata-shi, 950-2181 Japan.
a) E-mail: yamada@ie.niigata-u.ac.jp
b) E-mail: morisita@wave.ie.niigata-u.ac.jp
c) E-mail: yamaguch@ie.niigata-u.ac.jp

DOI: 10.1093/ietcom/e90–b.9.2288

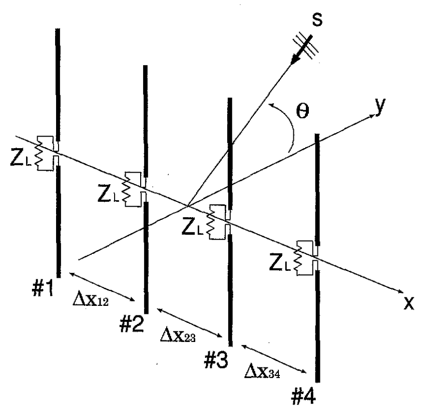

Fig. 1 DOA estimation with an N-element dipole array.

it works pretty well for some dipole arrays. Numerical and experimental results are presented in Sect. 4 to show the performance and limitation of the method.

2. Problem Formulation

For simplicity, we consider the DOA estimation problem of an N-element linear array as shown in Fig. 1 (a 4-element dipole array ($N = 4$) in this figure). We also assume that all the elements are the same and terminated by Z_L. When a plane wave impinges on the array at angle of θ, the received data vector of the array can be written by

$$\boldsymbol{i} = \boldsymbol{C}\boldsymbol{a}(\theta)s + \boldsymbol{n}, \tag{1}$$

where $\boldsymbol{i}$ and $\boldsymbol{n}$ are an N-dimensional vectors whose element corresponds to the terminal current and an additive noise of each array element, respectively. An N-dimensional vector $\boldsymbol{a}(\theta)$ and a s are a mode vector and a complex voltage of the incident wave, respectively. An $N \times N$ matrix $\boldsymbol{C}$ denotes the mutual coupling matrix of the array.

In this formulation, the array calibration problem becomes estimation problem of the coupling matrix $\boldsymbol{C}$. It can be precisely estimated when enough calibration dataset of the plane waves having known DOAs [2] is available. In the DOA estimation of plane wave incidence, the coupling matrix $\boldsymbol{C}$ should be estimated by the plane wave illumination to the array, hence we denotes the matrix as $\boldsymbol{C}_{\text{plane}}$ in the followings.

In this paper, we assume that each element is a half-wavelength dipole which acts as a quasi single-mode element, and also no coupling objects exists near the elements. In the next section, we describe the conventional mutual coupling matrix of the array and show the proposed compensation scheme.

3. The Mutual Coupling Matrix of the Array

3.1 The Impedance Matrix and Conventional Calibration Matrix

As discussed in [4], the induced voltages by the incident waves and terminal currents can be modeled by using the open-circuit voltages and terminal currents of the equivalent circuit of the array. When we denotes the voltage and the current vector as $\boldsymbol{v}$ and $\boldsymbol{i}$, respectively, we obtain

$$\boldsymbol{v} = (\boldsymbol{Z} + Z_L\boldsymbol{I})\boldsymbol{i}, \tag{2}$$

where $\boldsymbol{Z}$ is an $N \times N$ impedance matrix of the array, and $\boldsymbol{I}$ is the identity matrix. The current vector $\boldsymbol{i}$ corresponds to the terminal current vector in (1). Clearly, the open-circuit voltage vector $\boldsymbol{v}$, which corresponds to the ideal/uncoupled voltage vector, can be easily derived when the impedance matrix $\boldsymbol{Z}$ is known.

The mutual impedance matrix can be easily measured without employing the external reference plane-waves. Let us excite only the k-th element by V_0. The relation between the voltage vector $\boldsymbol{v}_k$ and the corresponding current vector $\boldsymbol{i}_k$ can be written by,

$$\boldsymbol{v}_k = V_0\boldsymbol{u}_i = (\boldsymbol{Z} + Z_L\boldsymbol{I})\boldsymbol{i}_k, \quad k = 1, \cdots, N, \tag{3a}$$

$$\boldsymbol{u}_k = [\underbrace{0, \cdots, 0}_{k-1}, 1, 0 \cdots, 0]^T, \tag{3b}$$

where T denotes transpose. $\boldsymbol{u}_k$ is an N dimensional vector whose the k-th element is 1 and the remaining elements are zeros. When each element is excited individually by $\boldsymbol{v}_1, \boldsymbol{v}_2, \cdots, \boldsymbol{v}_k$, we obtain

$$\boldsymbol{Z} + Z_L\boldsymbol{I} = V_0\boldsymbol{J}_{\text{delta}}^{-1}, \tag{4a}$$

$$\boldsymbol{J}_{\text{delta}} = [\boldsymbol{i}_1, \boldsymbol{i}_2, \cdots, \boldsymbol{i}_N]. \tag{4b}$$

The mutual impedance matrix can be measured by above equations. Note that the subscript "delta" is used here to denote that the matrix is measured by the delta-gap feed excitation of each element. The impedance matrix can also be measured by S-parameter measurement with a network analyzer.

From (2) and (1), we can define the mutual coupling matrix by

$$\boldsymbol{C}_{\text{delta}} = (\boldsymbol{Z} + Z_L\boldsymbol{I})^{-1}. \tag{5}$$

We also use the subscript "delta" to denote the matrix is estimated by the delta-gap feed excitation.

This calibration method is simple and clear, however, the estimated calibration matrix $\boldsymbol{C}_{\text{delta}}$ is often biased, even for the array of the half-wavelength dipoles. In this derivation, the open-circuit voltage of the elements is assumed to be independent from the other elements. Strictly speaking, this assumption only holds for ideal single-mode elements. In general, scattered waves by the adjacent general (quasi-) single-mode elements often affect to the open-circuit voltages of the others [5], [6], which cause estimation bias.

3.2 The Proposed Compensation Matrix

Main objective in this paper is development of a simple and an effective compensation technique. We can obtain the approximate calibration/coupling matrix, $\boldsymbol{C}_{\text{delta}}$, relative easily.

Then we focus on the consideration of accuracy improvement of the matrix $\boldsymbol{C}_{\text{delta}}$. As discussed in the previous subsection, main difference in the estimation between th $\boldsymbol{C}_{\text{delta}}$ and $\boldsymbol{C}_{\text{plane}}$ is the excitation of the elements. In the estimation of the matrix $\boldsymbol{C}_{\text{plane}}$, each element is excited uniformly by the plane wave. On the other hand, only the feed point of each element is excited by the delta-gap feed excitation in $\boldsymbol{C}_{\text{delta}}$. Then, current distribution on the elements in each excitation is slightly changed even when the array of the half-wavelength dipoles is employed [7].

Concept of the proposed modification is simple. The proposed compensation matrix is defined by the modification of the diagonal elements of the conventional coupling matrix $\boldsymbol{C}_{\text{delta}}$, which can be written by

$$\hat{\boldsymbol{C}}'(\zeta) = \boldsymbol{C}_{\text{delta}} - \zeta \boldsymbol{I}, \tag{6}$$

or

$$\hat{\boldsymbol{C}}(\rho) = (\rho \boldsymbol{I}) \odot \boldsymbol{C}_{\text{delta}}, \tag{7}$$

where ζ and ρ are compensation coefficients to decrease the difference between $\boldsymbol{C}_{\text{plane}}$ and $\boldsymbol{C}_{\text{delta}}$ due to the element excitation. Operator $\odot$ denotes the Hadamard matrix product (element-wise multiplication). The matrix $\hat{\boldsymbol{C}}'(\zeta)$ is defined by diagonal loading, while the matrix $\hat{\boldsymbol{C}}(\rho)$ is defined by diagonal weighting. Theoretical background of these matrices is shown in the next subsection.

In (7) (or (6)), we introduce the new unknown ρ (or ζ). Then, estimation of the parameter is the next problem. The superresolution techniques reveal their best performance when the data are well calibrated. This means that we can *estimate* the unknown parameter as well as the DOAs of the incident waves in the DOA estimation procedure, without any special measurement in advance. For example, when we apply the MUSIC algorithm [1] with the coupling matrix $\hat{\boldsymbol{C}}(\rho)$, the MUSIC spectrum for the DOAs and compensation coefficient can be modified by

$$P_{\text{MUSIC}}(\theta, \rho) = \frac{\boldsymbol{a}(\theta)^H \hat{\boldsymbol{C}}(\rho)^H \hat{\boldsymbol{C}}(\rho) \boldsymbol{a}(\theta)}{\boldsymbol{a}(\theta)^H \hat{\boldsymbol{C}}(\rho)^H \boldsymbol{E}_N \boldsymbol{E}_N^H \hat{\boldsymbol{C}}(\rho) \boldsymbol{a}(\theta)} \tag{8}$$

where a matrix $\boldsymbol{E}_N$ is the noise-subspace matrix defined by the eigenvectors corresponding minimum eigenvalues of the measured data covariance matrix [1].

The MUSIC spectrum is very sensitive to errors. The peak value of the spectrum tends to infinity in an ideal data of high SNR and large number of snapshots with precise calibration. Therefore, we can estimate the proper value of ρ, and more precise DOAs as well, to maximize the peak(s) of the spectrum by searching in θ and ρ. The estimation performance of the compensation coefficient ρ would be depends on the SNR and number of snapshots of the data. Since estimation of the compensation parameter will be failed with low SNR and/or few snapshots data set, we need a calibration with a plane wave incidence in advance for such applications. However, we only need the data of single source with *unknown* DOA because the DOA can be estimated by (8). Therefore the calibration measurement becomes simple in comparison with that for conventional calibration with the reference plane waves[2] having *known* DOAs.

3.3 Theoretical Background of the Proposed Compensation

As discussed in the previous subsection, the current distribution on each element causes the difference between the coupling matrix defined by $\boldsymbol{C}_{\text{plane}}$ and $\boldsymbol{C}_{\text{delta}}$. In this section, we employ the MoM to treat the effect of the current distribution. For simplicity, we assume that the N-element dipole array whose element is divided into M segments as an example. By applying the MoM, we obtain the following equations[12].

$$\begin{bmatrix} \boldsymbol{v}_1^{\text{mom}} \\ \boldsymbol{v}_2^{\text{mom}} \\ \vdots \\ \boldsymbol{v}_N^{\text{mom}} \end{bmatrix} = \begin{bmatrix} \boldsymbol{Z}_{11}^{\text{mom}} & \cdots & \boldsymbol{Z}_{1N}^{\text{mom}} \\ \boldsymbol{Z}_{21}^{\text{mom}} & \cdots & \boldsymbol{Z}_{2N}^{\text{mom}} \\ \vdots & \ddots & \vdots \\ \boldsymbol{Z}_{N1}^{\text{mom}} & \cdots & \boldsymbol{Z}_{NN}^{\text{mom}} \end{bmatrix} \begin{bmatrix} \boldsymbol{i}_1^{\text{mom}} \\ \boldsymbol{i}_2^{\text{mom}} \\ \vdots \\ \boldsymbol{i}_N^{\text{mom}} \end{bmatrix},$$

$$\boldsymbol{v}^{\text{mom}} = \boldsymbol{Z}^{\text{mom}} \boldsymbol{i}^{\text{mom}}, \tag{9a}$$

$$\boldsymbol{Y}^{\text{mom}} \boldsymbol{v}^{\text{mom}} = \boldsymbol{i}^{\text{mom}}, \tag{9b}$$

where $\boldsymbol{v}^{\text{mom}}$ and $\boldsymbol{i}^{\text{mom}}$ are an NM-dimensional induced voltage vector and a current vector caused by $\boldsymbol{v}^{\text{mom}}$, respectively. The vectors $\boldsymbol{v}_i^{\text{mon}}$ and $\boldsymbol{i}_i^{\text{mon}}$ $(i = 1, 2, \cdots, N)$ are an M dimensional voltage and current vectors for each elements, respectively. The matrix $\boldsymbol{Z}^{\text{mon}}$ is the $MN \times MN$ impedance matrix which can be divided by $M \times M$ submatrices, $\boldsymbol{Z}_{ij}^{\text{mon}}$, corresponding to each element. Note that the terminal impedance, Z_L, is added to the corresponding element of the $\boldsymbol{Z}_{ii}$. $\boldsymbol{Y}^{\text{mon}}$ is the admittance matrix defined by the inverse of $\boldsymbol{Z}^{\text{mon}}$.

Let us define the voltage and current distribution vector of the k-th array-element, $\boldsymbol{g}_k$ and $\boldsymbol{h}_k$, whose elements are normalized by their terminal voltage and current, respectively, as

$$\boldsymbol{v}_k^{\text{mon}} = \boldsymbol{h}_k v_k, \quad k = 1, 2, \cdots, N, \tag{10a}$$

$$\boldsymbol{i}_k^{\text{mon}} = \boldsymbol{g}_k i_k, \quad k = 1, 2, \cdots, N. \tag{10b}$$

Substituting the equations into (9b), we have

$$\begin{bmatrix} \boldsymbol{g}_1 i_1 \\ \boldsymbol{g}_2 i_2 \\ \vdots \\ \boldsymbol{g}_N i_N \end{bmatrix} = \boldsymbol{Y}^{\text{mom}} \begin{bmatrix} \boldsymbol{h}_1 v_1 \\ \boldsymbol{h}_2 v_2 \\ \vdots \\ \boldsymbol{h}_N v_N \end{bmatrix}. \tag{11}$$

The element corresponding to the terminal in $\boldsymbol{g}_k$ is equal to 1 due to the normalization. Therefore, the received $N \times 1$ terminal current vector $\boldsymbol{i}$ can be given by

$$\begin{aligned} \boldsymbol{i} &= [i_1, i_2, \cdots, i_N]^T \\ &= \begin{bmatrix} \boldsymbol{y}_{11,\text{term}}^{\text{mom}} \boldsymbol{h}_1 & \cdots & \boldsymbol{y}_{1N,\text{term}}^{\text{mom}} \boldsymbol{h}_N \\ \boldsymbol{y}_{21,\text{term}}^{\text{mom}} \boldsymbol{h}_1 & \cdots & \boldsymbol{y}_{2N,\text{term}}^{\text{mom}} \boldsymbol{h}_N \\ \vdots & \ddots & \vdots \\ \boldsymbol{y}_{N1,\text{term}}^{\text{mom}} \boldsymbol{h}_1 & \cdots & \boldsymbol{y}_{NN,\text{term}}^{\text{mom}} \boldsymbol{h}_N \end{bmatrix} \begin{bmatrix} v_1 \\ v_2 \\ \vdots \\ v_N \end{bmatrix} \\ &= \boldsymbol{C} \boldsymbol{v}, \end{aligned} \tag{12}$$

where $\boldsymbol{y}^{\text{mom}}_{k\ell,\text{term}}$ denotes an N dimensional row vector of $\boldsymbol{Y}^{\text{mon}}_{k,\ell}$ whose row corresponds to the terminal segment.

As shown in (12), the coupling matrix $\boldsymbol{C}$ can be expressed by

$$\boldsymbol{C} = \begin{bmatrix} \boldsymbol{y}^{\text{mom}}_{11,\text{term}}\boldsymbol{h}_1 & \cdots & \boldsymbol{y}^{\text{mom}}_{1N,\text{term}}\boldsymbol{h}_N \\ \boldsymbol{y}^{\text{mom}}_{21,\text{term}}\boldsymbol{h}_1 & \cdots & \boldsymbol{y}^{\text{mom}}_{2N,\text{term}}\boldsymbol{h}_N \\ \vdots & \ddots & \vdots \\ \boldsymbol{y}^{\text{mom}}_{N1,\text{term}}\boldsymbol{h}_1 & \cdots & \boldsymbol{y}^{\text{mom}}_{NN,\text{term}}\boldsymbol{h}_N \end{bmatrix}. \quad (13)$$

Estimation of $\boldsymbol{C}_{\text{plane}}$ is done with $\boldsymbol{h}_i = [1, 1, \cdots, 1]^T = \mathbf{1}$, while the estimation of $\boldsymbol{C}_{\text{delta}}$ is done with $\boldsymbol{h}_i = \boldsymbol{u}_{\text{term}}$, where the 'term' denotes the segment-number. The voltage distribution difference on the elements causes the difference between $\boldsymbol{C}_{\text{plane}}$ and $\boldsymbol{C}_{\text{delta}}$. The ideal coupling matrix $\boldsymbol{C}_{\text{plane}}$ can be approximated by using the adequate complex constants, w_d, w_p, as

$$\boldsymbol{C}_{\text{plane}} = w_d \boldsymbol{C}_{\text{delta}} + w_d \begin{bmatrix} \boldsymbol{y}^{\text{mom}}_{11,\text{term}}\boldsymbol{h}_{\text{diff}} & \cdots & \boldsymbol{y}^{\text{mom}}_{1N,\text{term}}\boldsymbol{h}_{\text{diff}} \\ \boldsymbol{y}^{\text{mom}}_{21,\text{term}}\boldsymbol{h}_{\text{diff}} & \cdots & \boldsymbol{y}^{\text{mom}}_{2N,\text{term}}\boldsymbol{h}_{\text{diff}} \\ \vdots & \ddots & \vdots \\ \boldsymbol{y}^{\text{mom}}_{N1,\text{term}}\boldsymbol{h}_{\text{diff}} & \cdots & \boldsymbol{y}^{\text{mom}}_{NN,\text{term}}\boldsymbol{h}_{\text{diff}} \end{bmatrix}, \quad (14a)$$

$$\boldsymbol{h}_{\text{diff}} = \mathbf{1} - \frac{w_p}{w_d}\boldsymbol{u}_{\text{term}}. \quad (14b)$$

This procedure is similar to Ref. [7]. In Ref. [7], the author has introduced the current distribution function of the elements to estimate the *precise* calibration matrix. On the other hand, we just focus on the difference between $\boldsymbol{C}_{\text{plane}}$ and $\boldsymbol{C}_{\text{delta}}$ and approximate it with few unknowns to derive a simple *compensation* matrix.

Obviously dominant terms in (13) are the diagonal terms, hence by adjusting the weights, w_d and w_p, we can approximate the second matrix in the right side of (14a) as a diagonal matrix. Furthermore, difference among the elements of the diagonal matrix will be small for arrays of the same elements with the moderate element separation. When these assumptions/approximations hold, we can obtain

$$\boldsymbol{C}_{\text{plane}} \simeq w_d(\boldsymbol{C}_{\text{delta}} + \zeta \boldsymbol{I}). \quad (15)$$

Clearly, we can omit the complex coefficient w_d because it does not affect the calibration/compensation performance. This is the theoretical background of the approximations in (6). Physical interpretation of the approximation in (15) can be also derived by decomposing the coupling phenomenon as multiple reflections. See [13] for details. Apparently, these assumptions cannot hold for arrays with closely spaced elements, which will be demonstrated in the next section.

Main objective in this paper is derivation of a simple compensation technique based on the impedance matrix. In the expression of (6), we should carry out the two-dimensional search in amplitude and phase, or real and imaginary, of ζ. This can be further simplified when the coupling effect is not severe. Since we employ the (quasi-) single-mode elements, difference of the initial current distribution on the elements will be small. Then, we have $|\tilde{\zeta}| \ll 1$, where $\tilde{\zeta}$ is the ζ normalized by the corresponding diagonal element in $\boldsymbol{C}_{\text{delta}}$. In addition, for the arrays with the moderate element separation, the difference among the diagonal elements of $\boldsymbol{C}_{\text{delta}}$ will be small. In such a case, the following expression will be also applicable,

$$\boldsymbol{C}_{\text{plane}} \propto (\rho \boldsymbol{I}) \odot \boldsymbol{C}_{\text{delta}}. \quad (16)$$

This corresponds to the expression of the proposed compensation matrix in (7). For the arrays of (quasi-)single-mode elements such as half-wavelength dipoles, we found in the numerical simulations that the further approximations as $|\rho| \simeq 1$ is effective. This means that we can still obtain a better compensation performance with $\boldsymbol{C}_{\text{delta}}$ by phase adjustment of the diagonal elements in $\boldsymbol{C}_{\text{delta}}$. In this case, the MUSIC spectrum in (8) becomes

$$P_{\text{MUSIC}}(\theta, \phi_\rho) = \frac{\boldsymbol{a}(\theta)^H \hat{\boldsymbol{C}}(\phi_\rho)^H \hat{\boldsymbol{C}}(\phi_\rho) \boldsymbol{a}(\theta)}{\boldsymbol{a}(\theta)^H \hat{\boldsymbol{C}}(\phi_\rho)^H \boldsymbol{E}_N \boldsymbol{E}_N^H \hat{\boldsymbol{C}}(\phi_\rho) \boldsymbol{a}(\theta)}, \quad (17a)$$

$$\hat{\boldsymbol{C}}(\phi_\rho) = (e^{j\phi_\rho} \boldsymbol{I}) \odot \boldsymbol{C}_{\text{delta}}, \quad (17b)$$

where ϕ_ρ is the phase of ρ.

As shown in (17a), the DOA estimation by the MUSIC with coupling error compensation can be realized by the simple 2D search on θ and ϕ_ρ when the assumptions/approximations are hold. For the 2D algorithms having heavy computational loads, it may be difficult to realize real-time processing. However, the compensation parameter, ρ or ϕ_ρ, is stable in time if the array is unchanged. Hence, the 2D estimation is required only in the initial estimation. Once the parameter ρ is estimated, we can use the estimated ρ throughout the DOA estimations.

As discussed in this section, the proposed compensation matrix is obtained by the rough approximations, then we might say it would be the empirical formula. In the next section, we will verify availability and limitation of the proposed compensation technique by using the array of half-wavelength dipoles which often utilized in practical applications.

4. Numerical and Experimental Results

4.1 Numerical Results

Numerical verification of the proposed technique is carried out by using an array of 4-element dipoles as shown in Fig. 1. The array parameters are also listed in Table.1. The (coupled) received data are calculated numerically by the

Table 1 Array parameters.

Frequency (Wavelength: λ)	2.4 GHz (λ=12.5 cm)
Element length	5.8 cm (0.464 λ)
Element radius	0.5 mm
Terminal Impedance (Z_L)	50 Ω
Number of the elements (N)	4

method of moments.

The first step in the proposed compensation is the estimation of the conventional calibration matrix $\boldsymbol{C}_{\text{delta}}$ in (5). The terminal currents $\boldsymbol{i}_k$ derived by the MoM are used for the calculation in (4a). Next step is the estimation of the optimal compensation coefficient of ρ in (7). This can be done by using the observed signals in the DOA estimation. When we employed the MUSIC algorithm, DOA of the incident waves and corresponding ρs can be estimated by (8). For multiple wave data, the estimated ρ of each wave may not coincides with each other because of the approximations in the proposed compensation. In such a case, the average value of them would be adopted. Once the optimal ρ is estimated, we can determine the optimal $\hat{\boldsymbol{C}}(\rho)$ in (7). The following estimation can be done by using the constant compensation matrix $\hat{\boldsymbol{C}}(\rho)$.

The first example is the uniform linear array (ULA) with element separation of 0.48λ ($\Delta x_{ij} = 0.48\lambda$ in Fig. 1). The $\boldsymbol{C}_{\text{delta}}$ is also derived numerically by the method of moments by the procedure described in Sect. 3.1. To show the error compensation performance itself, this numerical evaluation is done with no noise (infinite SNR), which is equivalent to the infinite number of snapshots in finite SNR. Figure 2 shows the $P_{\text{MUSIC}}(\theta, \phi_\rho)$ spectrum in (17a). Here we use the data of one incident wave from $\theta_0 = 50°$ in this estimation. The estimated peak in Fig. 2 is located at $(\theta, \phi_\rho) = (50°, -9.3°)$. As shown in this figure, the maximum of the spectrum appears at the true DOA of the incident wave. This means that the peak characteristic of the MUSIC spcetrum can be recovered by the suitable diagonal weight in $\boldsymbol{C}_{\text{delta}}$. Idealy, the peak value becomes infinite for the no noise data when the data are precisely calibrated. However, the peak value is limited in this example. This is due to the approximation accuracy of the proposed compensation scheme. The DOA estimation results for the one-wave incidence at several DOAs and their DOA estimation errors are shown in Figs. 3(a) and (b), where 'Raw Data,' 'Conventional,' and 'Proposed' show the estimated results without compensation, those with $\boldsymbol{C}_{\text{delta}}$ compensation by (5), and those with $\hat{\boldsymbol{C}}(\phi_\rho)$ compensation by (17b), respectively. Note that the eigenvectors corresponding to the zero eigenvalues in the covariance matrix of the data are the columns of $\boldsymbol{E}_N$ in (17a) because of no noise. In the calibration with $\hat{\boldsymbol{C}}((\phi_\rho))$, the estimated value of $\rho = e^{-j\phi_\rho}$ in Fig. 2 is used throughout the DOA estimations. As shown in these figures, the peak property of the MUSIC algorithm is improved and the DOA estimation error can be decreased effectively by the proposed compensation technique. Note that the DOA estimation error becomes almost zero by the proposed simple compensation.

In the approximation in (15), we assume that the off diagonal elements in the second matrix in the right side of (14b) are small and whose diagonal elements have almost the same value. Clearly, these assumptions are violated for the arrays of closely spaced elements. Figures 4 and 5 show the results of the 4-element ULA with element separation of 0.2λ. Although the DOA estimation errors can be decreased compared with those by the conventional calibration, there still remain biases. In addition, the peaks of the MUSIC

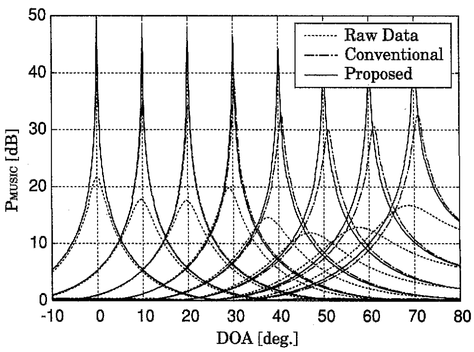

(a) MUSIC Spectrum

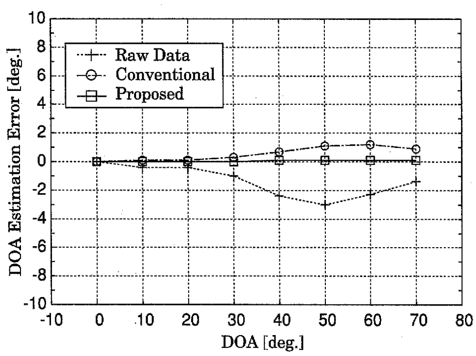

(b) DOA Estimation Error

Fig. 3 DOA estimation results and estimation errors by the MUSIC algorithm. $N = 4$, $\Delta x_{12} = \Delta x_{23} = \Delta x_{34} = 0.48\lambda$, SNR $= \infty$(no noise).

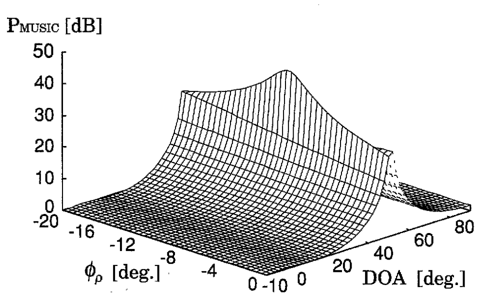

Fig. 2 The DOA and compensation coefficient estimation by $P_{\text{MUSIC}}(\theta, \phi_\rho)$. $N = 4$, $\Delta x_{12} = \Delta x_{23} = \Delta x_{34} = 0.48\lambda$, $\theta_0 = 50°$, SNR $= \infty$(no noise).

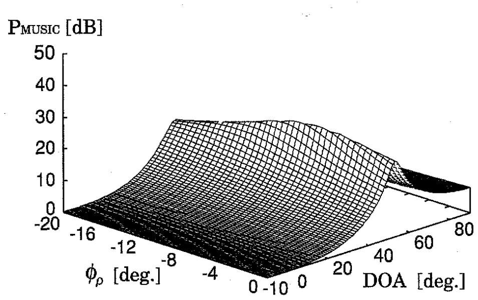

Fig. 4 The DOA and compensation coefficient estimation by $P_{\text{MUSIC}}(\theta, \phi_\rho)$. $N = 4$, $\Delta x_{12} = \Delta x_{23} = \Delta x_{34} = 0.2\lambda$, $\theta_0 = 50°$, SNR $= \infty$(no noise).

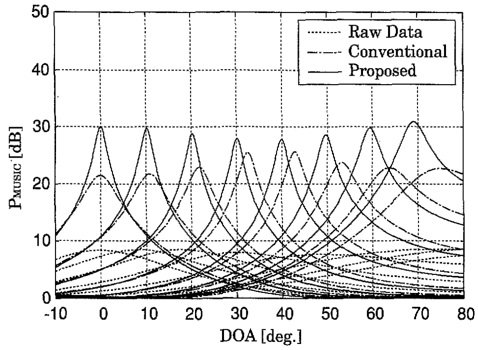

(a) MUSIC Spectrum

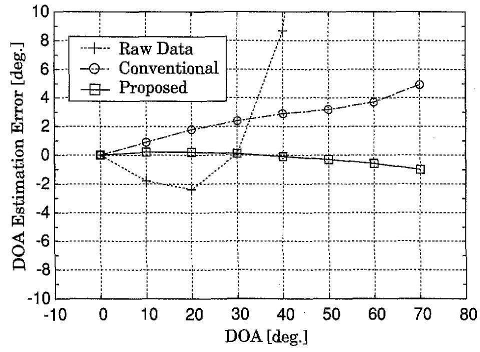

(b) DOA Estimation Error

Fig. 5 DOA estimation results and estimation errors by the MUSIC algorithm. $N = 4$, $\Delta x_{12} = \Delta x_{23} = \Delta x_{34} = 0.2\lambda$, SNR = ∞(no noise).

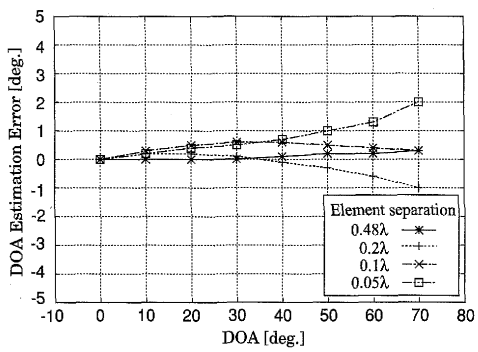

Fig. 6 Estimated DOA errors with ULAs having various element separations. $N = 4$, $\theta_0 = 50°$, SNR = ∞(no noise).

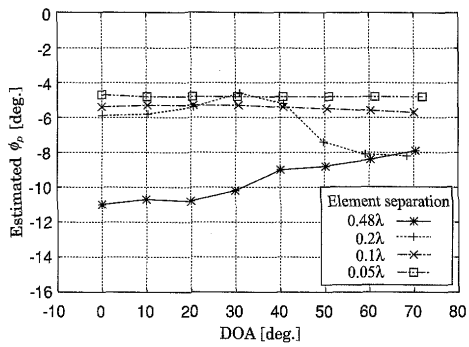

Fig. 7 Estimated ϕ_ρ with ULAs of various DOAs and element separations. $N = 4$, SNR = ∞(no noise).

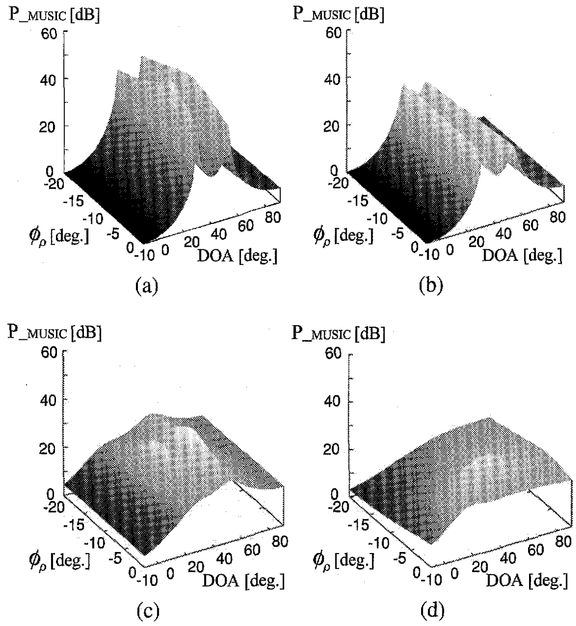

Fig. 8 DOA and compensation coefficient estimation by the $P_{MUSIC}(\theta, \phi_\rho)$ with finite SNR/snapshots. $N = 4$, $\theta_1 = 30°$, $\theta_2 = 50°$, 50 snapshots. (a) SNR=30 dB, 0.48λ element separation, (b) SNR=10 dB, 0.48λ element separation, (c) SNR=10 dB, 0.2λ element separation, (d) SNR=10 dB, 0.1λ element separation.

spectrum cannot be recovered enough. As shown in this example, the proposed technique is not effective for the arrays having severe mutual coupling. This is the limitation of the proposed compensation scheme.

The estimated DOAs by the MUSIC algorithm with ULAs having various element separations are shown in Fig. 6. The estimated value of ϕ_ρ by single wave incidence at $\theta_0 = 50°$ is used in each estimation. It is clear that good error compensation can be realized with the array of 0.48λ element separation. When the inter element separation becomes 0.2λ or less, we cannot compensate the DOA bias by the proposed scheme. This shows the limitation of this simple parametric compensation technique.

In the above simulations, the single wave incidence data at $\theta = 50°$ are used for the optimal compensation coefficient estimation. DOA dependence of the estimated value ϕ_ρ must be examined. The estimated ϕ_ρ in various DOAs and element separations are plotted in Fig. 7. Since the compensation coefficient, ϕ_ρ, is derived by rough approximations, then estimated ϕ_ρ slightly changes in DOA of the incident wave. Figure 7 shows that almost 3° difference occurs for 0.48λ and 0.2λ separation. The DOA estimation errors with these coefficients were also examined numerically. Difference of the DOA estimation error was less than 0.1°, hence, we could say that the ϕ_ρ estimation is robust in DOA.

In the actual applications, we only have noisy data of the finite number of snapshots. Furthermore, the observed data will often contain multiple incident waves. Figures 8(a)~(d) show the examples of the 2 wave incidence with 50 snapshots. Each peak can be clearly resolved in Fig. 8(a) since the SNR is high (30 dB) and DOAs of the two waves are separated enough. However the peaks become dull for the low SNR case shown in Fig. 8(b). These are the estimated results with the array of 0.48λ separation.

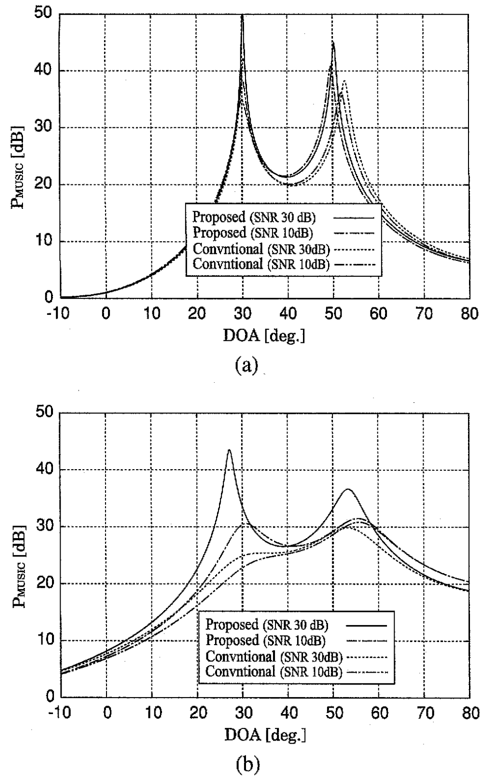

Fig. 9 The MUSIC spectrum estimated by the finite SNR/snapshot data. $N = 4$, $\theta_1 = 30°$, $\theta_2 = 50°$, 50 snapshots. (a) 0.48λ element separation, (b) 0.48λ element separation.

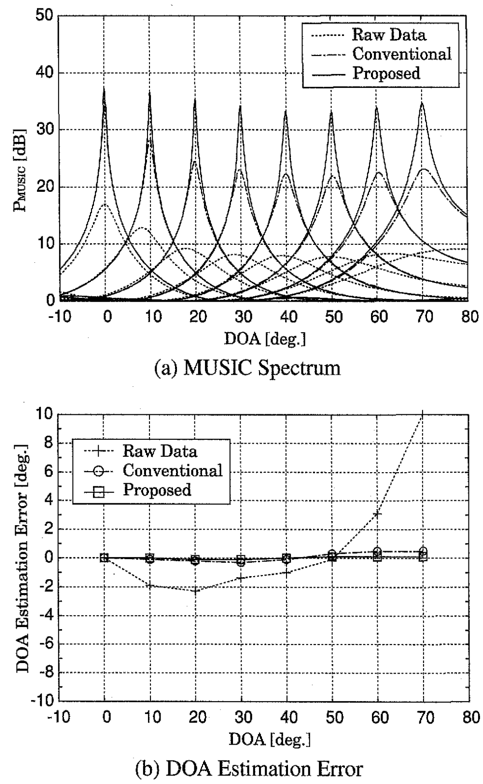

Fig. 10 DOA estimation results and estimation errors by the MUSIC algorithm. $N = 4$, $\Delta x_{12} = \Delta x_{34} = 0.65\lambda$, $\Delta x_{23} = 0.2\lambda$, SNR = ∞(no noise).

The estimated DOAs by using average value of detected two ϕ_ρs are also shown in Fig. 9(a). Good error compensation property is still realized in these dataset. The compensation performance deteriorates in small element separation as shown in Fig. 8(c) and (d). The two peaks can be resolved in Fig. 8(c), however, the estimated DOAs by the obtained coefficient is biased (Fig. 9(b)). Furthermore, we cannot resolve two waves in Fig. 8(d). This means that we cannot estimate the proper ϕ_ρ. To make the error compensation model simple, we apply relative rough approximations/assumptions, therefore the proposed technique is not applicable to the array with small element separation. However the technique is still work properly for the noisy finite snapshot data including multiple sources when we employ the array of almost half-wavelength element separation.

Additional feature of the proposed compensation technique to be noted is concerned with the array geometry. No information on the array geometry is imposed in derivation of the proposed technique, then the technique is applicable when the assumptions/approximations hold. Figures 10(a) and (b) show the results of the MUSIC spectrum and the estimated DOA errors by the 4-element array with $\Delta x_{12} = \Delta x_{34} = 0.65\lambda$ and $\Delta x_{23} = 0.2\lambda$. As can be seen in these figures, good calibration performance can be realized by the proposed calibration technique.

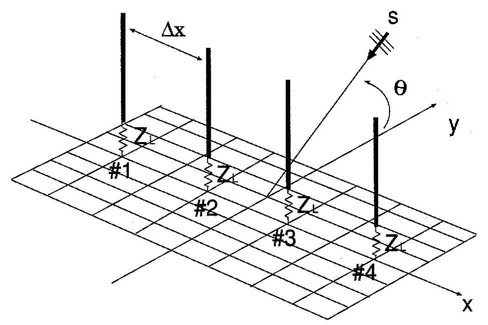

Fig. 11 DOA estimation with 4-element monopole array.

4.2 Experimental Results

Availability of the proposed calibration was also verified by the experiments. The experiment was done with a network analyzer in an anechoic chamber. The array employed in the experiment was the 4-element uniform monopole array on the finite ground plane as shown in Fig. 11. The array parameters are listed in Table 2. The size of the ground plane was $2\lambda \times 3.5\lambda$ whose edges were rounded so as to decrease effect by the edge/corner scatterings. The estimation procedure is the same as described in the previous subsection. The impedance matrix required in the first step can be easily derived by the measured S-parameters with the network analyzer and Z_L is a known value, then we can obtain $\boldsymbol{C}_{\text{delta}}$ in (5).

Figure 12 shows the estimated $P_{\text{MUSIC}}(\theta, \phi_\rho)$ spectrum for the one-wave incidence from $\theta_0 = 50°$ with 1 snap-

Table 2 Array parameters for the experiment.

Frequency (Wavelength: λ)	2.4 GHz (λ=12.5 cm)
Element length	3.11 cm (0.249 λ)
Element radius	0.5 mm
Terminal Impedance (Z_L)	50 Ω
Number of the elements (N)	4
Element Separation (Δx)	6.22 cm (0.498λ)

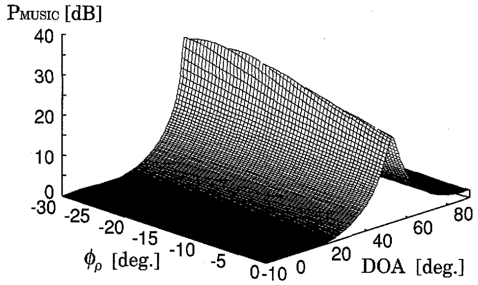

Fig. 12 DOA and compensation coefficient estimation by $P_{\text{MUSIC}}(\theta, \phi_\rho)$. $N = 4$, $\Delta x = 0.498\lambda$, $\theta_0 = 50°$, 1 snapshot.

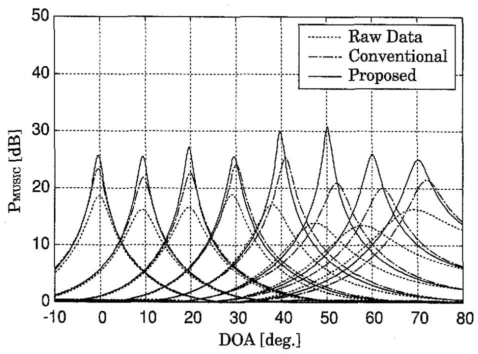

(a) MUSIC Spectrum

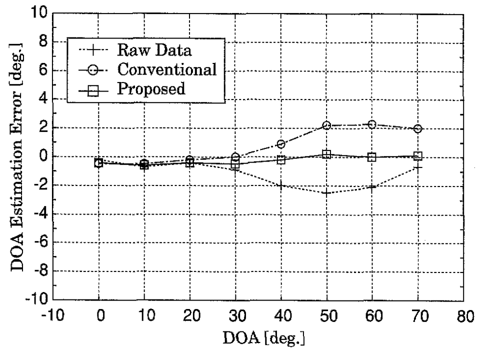

(b) DOA Estimation Error

Fig. 13 DOA estimation results and estimation errors by the MUSIC algorithm. $N = 4$, $\Delta x = 0.498\lambda$, 1 snapshot.

shot data. The peak was detected at around $(\theta, \phi_\rho) \simeq (50.2°, -24.4°)$. Since the estimation was carried out with only one snapshot data, then the estimated peak became dull and position of the detected peak would be slightly biased due to the noise. In addition, although we tried to decrease the effect of the edge scattering by the ground plane, the remaining scattered waves by the edges would also cause bias of the peak. It will be improved when many-snapshot data and a large-sized ground plane are available. The estimated MUSIC spectrum and DOA errors are shown in Figs. 13(a) and (b). Improvement of the peak property in the MUSIC spectrum is relative small as we expected. This was due to the noise and the ground plane effect. However, as shown in Fig. 13(b), the DOA estimation error can be decreased effectively by the proposed technique. These results show that the proposed technique is available for the monopole-array with half-wavelength separation.

5. Conclusions

In this paper, we propose a simple array calibration technique based on the impedance matrix of the array. The proposed compensation technique is derived by the approximations to decrease the difference between the exact mutual coupling matrix and the matrix derived by the open-circuit technique. We show with some approximations and assumptions that accuracy of the mutual coupling matrix derived by the open-circuit technique can be easily improved by adjusting its diagonal elements.

Numerical and experimental results of the 4-element arrays are provided to show validity and limitations of the proposed technique. Although we apply many assumptions/approximations to derive the technique, the technique is applicable for usual dipole/monopole arrays of quasi single-mode elements with half-wavelength spacings.

Availability for arrays of the other single-mode elements, calibration performance in various SNRs, and still remains to be considered. Effect of the size ground plane is also one of the important problems to be clear for practical applications. They will be done in near future.

References

[1] R.O. Schmidt, "Multiple emitter location and signal parameter estimation," IEEE Trans. Antennas Propag., vol.AP-34, no.3, pp.276–280, March 1986.
[2] C.M. S. See, "Sensor array calibration in the presence of mutual coupling and unknown sensor gains and phases," Electron. Lett., vol.3, vol.30, no.5, pp.373–374, March 1994.
[3] B. Lindmark, "Comparison of mutual coupling compensation to dummy colums in adaptive antenna system," IEEE Trans. Antennas Propag., vol.53, no.4, pp.1332–1336, April 2005.
[4] I.J. Gupta and A.A. Ksienski, "Effect of mutual coupling on the performance of adaptive arrays," IEEE Trans. Antennas Propag., vol.AP-31, no.5, pp.785–791, Sept. 1983.
[5] R.S. Adve and T.K. Sarkar, "Compensation for the effects of mutual coupling on direct data domain adaptive algorithm," IEEE Trans. Antennas Propag., vol.48, no.1, pp.86–94, Jan. 2000.
[6] H.T. Hui, "Reducting the mutual coupling effect in adaptive nulling using a re-defined mutual impedance," IEEE Trans. Microwave and Wireless Component Letters, vol.12, no.5, pp.178–180, May 2002.
[7] H.T. Hui, "A practical approach to compensate for the mutual coupling effect in an adaptive dipole array," IEEE Trans. Antennas Propag., vol.52, no.5, pp.1262–1269, May 2004.
[8] C.K.E. Lau, R.S. Adve, and T.K. Sarkar, "Minimum norm mutual coupling compensation with application in direction of arrival estimation," IEEE Trans. Antennas Propag., vol.52, no.8, pp.2034–2041, Aug. 2004.
[9] Q. Yuan, Q. Chen, and K. Sawaya, "Accurate DOA estimation using array antenna with arbitrary geometry," IEEE Trans. Antennas Propag., vol.53, no.4, pp.1352–1357, April 2005.

[10] K.R. Dandekar, H. Ling, and G. Xu, "Experimental study of mutual coupling compensation in smart antenna applications," IEEE Trans. Wireless Communications, vol.1, no.3, pp.480–487, July 2002.
[11] D. Segovia-Vargas, R. Martin-Cuerdo, and M. Sierra-Perez, "Mutual coupling effects correction in microstrip arrays for direction-of-arrival (doa) estimation," IEE Proc. Microwaves, Antennas and Propagation, vol.149, no.2, pp.113–118, April 2002.
[12] T.K. Sarkar, M.C. Wicks, M.S. Palma, and R.J. Bonneau, Smart Antennas, Wiley-Interscience, 2003.
[13] H. Yamada, M. Morishita, and Y. Yamaguchi, "Simple calibration technique for arrays with single-mode elements based on mutual impedance matrix," Proc. 2006 International Symposium on Antennas and Propagations (ISAP'06), CD-ROM, Nov. 2006.

Hiroyoshi Yamada received the B.E, M.E. and Dr.Eng. degrees in electronic engineering from Hokkaido University, Sapporo, Japan, in 1988, 1990 and 1993, respectively. In 1993, he joined the Faculty of Engineering, Niigata University, where he is an associate professor. From 2000 to 2001, he was a Visiting Scientist at the Jet Propulsion Laboratory, California Institute of Technology, Pasadena. His current interests include superresolution techniques, array signal processing, and microwave remote sensing and imaging. Dr. Yamada is a member of the IEEE.

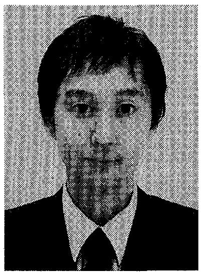

Masayuki Morishita received a B.E. degree in information engineering from Niigata University, Niigata, Japan, in 2006. He is now a graduate student pursuing an M.E. degree in Mathematics, Electronics and Information Engineering at Niigata University, where he is researching and developing adaptive array and array calibration technique.

Yoshio Yamaguchi received a B.E. degree in electronics engineering from Niigata University in 1976 and M.E. and Dr. Eng. degrees from the Tokyo Institute of Technology in 1978 and 1983, respectively. In 1978, he joined the Faculty of Engineering, Niigata University, where he is a professor. During 1988 and 1989, he was a research associate at the University of Illinois, Chicago. His interests include the propagation characteristics of electromagnetic waves in a lossy medium, radar polarimetry, and microwave remote sensing and imaging. Dr. Yamaguchi is a fellow of the IEEE.